Biosci. Rep. (2013) / **33** / art:e00022 / doi 10.1042/BSR20120115

OPEN ACCESS

Original Paper

Bioscience Reports

www.bioscirep.org

Bioscience Reports

# The kinetic properties of a human PPIP5K reveal that its kinase activities are protected against the consequences of a deteriorating cellular bioenergetic environment

Jeremy D. WEAVER, Huanchen WANG and Stephen B. SHEARS[1]

Inositol Signaling Group, Laboratory of Signal Transduction, National Institute of Environmental Health Sciences, NIH, DHHS, Research Triangle Park, P.O. Box 12233, NC 27709, U.S.A.

**Synopsis**

We obtained detailed kinetic characteristics – stoichiometry, reaction rates, substrate affinities and equilibrium conditions – of human PPIP5K2 (diphosphoinositol pentakisphosphate kinase 2). This enzyme synthesizes 'high-energy' *PP*-Ins*P*s (diphosphoinositol polyphosphates) by metabolizing Ins$P_6$ (inositol hexakisphosphate) and 5-Ins$P_7$ (5-diphosphoinositol 1,2,3,4,6-pentakisphosphate) to 1-Ins$P_7$ (1-diphosphoinositol 2,3,4,5,6-pentakisphosphate) and Ins$P_8$ (1,5-bis-diphosphoinositol 2,3,4,6-tetrakisphosphate), respectively. These data increase our insight into the PPIP5K2 reaction mechanism and clarify the interface between PPIP5K catalytic activities and cellular bioenergetic status. For example, stochiometric analysis uncovered non-productive, substrate-stimulated ATPase activity (thus, approximately 2 and 1.2 ATP molecules are utilized to synthesize each molecule of 1-Ins$P_7$ and Ins$P_8$, respectively). Impaired ATPase activity of a PPIP5K2-K248A mutant increased atomic-level insight into the enzyme's reaction mechanism. We found PPIP5K2 to be fully reversible as an ATP-synthase *in vitro*, but our new data contradict previous perceptions that significant 'reversibility' occurs *in vivo*. PPIP5K2 was insensitive to physiological changes in either [AMP] or [ATP]/[ADP] ratios. Those data, together with adenine nucleotide kinetics (ATP $K_m = 20–40\ \mu$M), reveal how insulated PPIP5K2 is from cellular bioenergetic challenges. Finally, the specificity constants for PPIP5K2 revise upwards by one-to-two orders of magnitude the inherent catalytic activities of this enzyme, and we show its equilibrium point favours 80–90% depletion of Ins$P_6$/5-Ins$P_7$.

*Key words:* bis-diphosphoinositol tetrakisphosphate, cellular energy homoeostasis, diphosphoinositol pentakisphosphate, diphosphoinositol polyphosphate, inositol pyrophosphate, inositol 1,3,4-trisphosphate 5/6-kinase (ITPK1)

Cite this article as: Weaver, J.D., Wang, H. and Shears, S.B. (2013) The kinetic properties of a human PPIP5K reveal that its kinase activities are protected against the consequences of a deteriorating cellular bioenergetic environment. Biosci. Rep. **33**(2), art:e00022.doi:10.1042/BSR20120115

## INTRODUCTION

*PP*-Ins*P*s [diphosphoinositol polyphosphates, such as 1-Ins$P_7$ (1-diphosphoinositol 2,3,4,5,6-pentakisphosphate), 5-Ins$P_7$ (5-diphosphoinositol 1,2,3,4,6-pentakisphosphate) and Ins$P_8$ (1,5-bis-diphosphoinositol 2,3,4,6-tetrakisphosphate); see Figure 1] have been shown to regulate diverse cellular processes such as vesicle trafficking, exocytosis, cytoskeletal dynamics, apoptosis, environmental stress response and insulin secretion and signalling (reviewed in [1–6]). Research into the mechanisms of action of the *PP*-Ins*P*s has identified a cyclin/cyclin kinase 'receptor' in yeast that is allosterically regulated by 1-Ins$P_7$ [7]. There is also evidence that 5-Ins$P_7$ can regulate cell-signalling by competing with PtdIns(3,4,5)$P_3$ for binding to pleckstrin homology domains [8]. Finally, *PP*-Ins*P*s have been reported to

**Abbreviations used:** DIPP, diphosphoinositol-polyphosphate phosphohydrolase; DTT, dithiothreitol; GST, glutathione transferase; Ins*P*, inositol phosphate; Ins$P_3$, inositol 1,3,4-trisphosphate; Ins$P_4$, inositol 1,3,4,5-tetrakisphosphate; Ins$P_5$, inositol 1,3,4,5,6-pentakisphosphate; Ins$P_6$, inositol hexakisphosphate; 1-Ins$P_7$, 1-diphosphoinositol 2,3,4,5,6-pentakisphosphate; 5-Ins$P_7$, 1-diphosphoinositol 2,3,4,5,6-pentakisphosphate; Ins$P_8$, 1,5-bis-diphosphoinositol 2,3,4,6-tetrakisphosphate; Ins$S_6$, inositol hexasulphate; IP6K, inositol hexakisphosphate kinase; ITPK1, inositol 1,3,4-trisphosphate 5/6-kinase; NCBI, National Center for Biotechnology Information; *PP*-Ins*P*s, diphosphoinositol polyphosphates; PPIP5K, diphosphoinositol pentakisphosphate kinase; PPIP5K2$^{KD}$, human diphosphoinositol pentakisphosphate kinase 2 kinase domain.

[1] To whom correspondence should be addressed (email Shears@niehs.nih.gov).

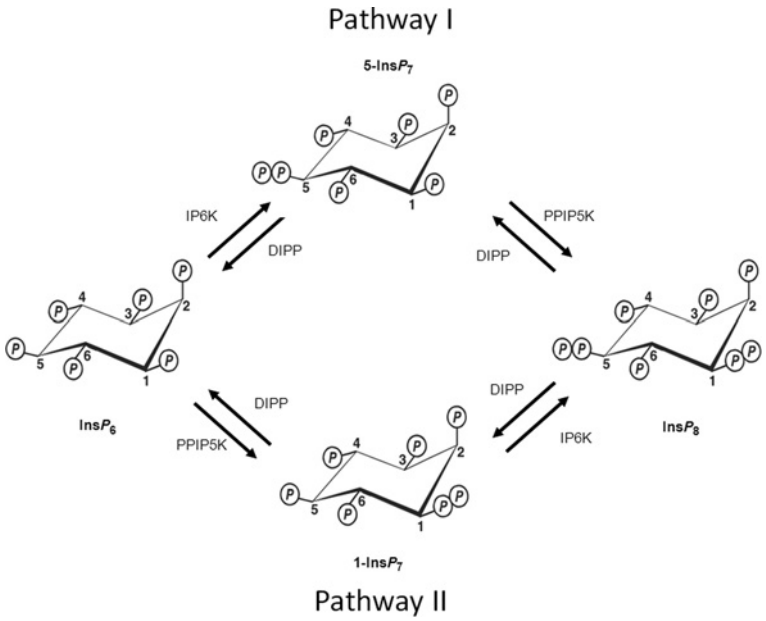


**Figure 1 Pathways of enzymatic synthesis of *PP*-Ins*P*s**

Figure modified from Shears 2009 [5]. The IP6Ks (myoinositol hexakisphosphate kinase; Kcs1 in yeast [48]), of which there are three isoforms in mammals, IP6K1, IP6K2 and IP6K3 [26,48,52], phosphorylate Ins$P_6$ and 1-Ins$P_7$ at the 5 position [41,53]. The PPIP5Ks (Vip1 in yeast [21]), of which there are two isoforms in mammals, PPIP5K1 and PPIP5K2 [18,19], phosphorylate Ins$P_6$ and 5-Ins$P_7$ at the 1 position [20,41]. Thus, the concerted actions of the IP6Ks and the PPIP5Ks leads to two routes of synthesis to Ins$P_8$, which are designated pathway I and pathway II after Padmanabhan *et al.* [17]. The diphosphate groups that are added by these kinases are hydrolysed by a family of *PP*-Ins*P* phosphohydrolases (DIPPs) [44,45].

promote the diphosphorylation of certain proteins thereby regulating inherent protein activities and protein/protein interactions [9–11]. Each of these proposed mechanisms of action of the *PP*-Ins*P*s are based upon a fundamental principle in signal transduction: their cellular levels are altered in a predictable manner in response to a specific intracellular or extracellular stimulus. For example, levels of 1-Ins$P_7$ are elevated during nutrient stress in yeast [7]. Total Ins$P_7$ levels also increase substantially following the addition of growth factors to cells that have been serum-starved overnight [8]. As for Ins$P_8$, its levels are elevated when cells are subjected to either hyperosmotic stress or a thermal challenge [12,13]. There are other circumstances that cause Ins$P_7$ and Ins$P_8$ levels to decrease, such as following oxidative stress [14]. Finally, Ins$P_8$ concentration decreases during bioenergetic stress [15].

It is because of all of these signalling activities that there is a need to characterize how the turnover of *PP*-Ins*P*s is regulated in intact cells. As with any signal transduction cascade, in order to understand its dynamic behaviour *in vivo*, it is critical to determine the kinetic parameters of its constituent signalling enzymes [16,17]. Such information – enzyme stoichiometry, reaction rates, substrate affinities and equilibrium conditions – helps us to understand the regulation of product generation as well as substrate depletion. In the current study, we provide new information concerning these properties of a PPIP5K (diphosphoinositol pentakisphosphate kinase), an enzyme that phosphorylates Ins$P_6$ (inositol hexakisphosphate) and 5-Ins$P_7$ to 1-Ins$P_7$ and Ins$P_8$, respectively (Figure 1).

Mammalian cells express two PPIP5Ks: types 1 and 2 that are 160 and 138 kDa, respectively [18,19]. The expression and purification of recombinant enzymes of such a large size are problematic. Fortunately, these are modular proteins; the N-terminal one-third of each of these proteins contains their kinase domain [18,20,21], following which is a centrally located PtdIns(3,4,5)$P_3$-binding module [22]. The active sites of these two kinase domains appear to be structurally and catalytically indistinguishable [18,20]; the relatively small number of residues elsewhere in these domains that are dissimilar are confined to the protein surface that is distal to the active site [20]. Thus, using the kinase domain of human PPIP5K2$^{KD}$ (PPIP5K2 kinase domain) as a model, we have now characterized the kinetic properties of this class of enzyme.

For an ATP-dependent kinase such as IP6K (inositol hexakisphosphate kinase) or PPIP5K, its activity may not solely depend upon the concentrations of inositol phosphate substrates. There is growing interest in the possibility that changes in the levels of adenine nucleotides may also be of importance in regulating IP6K and PPIP5K activity *in vivo* [1,2,5,6]. This idea has taken support from the evidence that bioenergetic homoeostasis interfaces with *PP*-Ins*P* turnover and cell signalling [15,23–26]. For example, some experiments indicate that bioenergetic health sets the cellular levels of *PP*-Ins*P*s [15,24–26]. Other work [23] indicates that

it is bioenergetic status that is regulated by the *PP*-Ins*P*s. One of the goals of the current study was to increase our understanding of the role of PPIP5K in this complex inter-relationship between signalling and metabolism.

Interest in the possibility of a link between cellular bioenergetics and *PP*-Ins*P* turnover began with the recognition that these molecules contain high-energy phosphoanhydride bonds that undergo rapid turnover *in vivo* [27,28]. Subsequently, in what was a startling exception for kinases in general [29], and inositol phosphate kinases in particular [30], a high $K_m$ (>1 mM) of the IP6K for ATP was determined [26]. IP6Ks were further shown to have a similarly high $K_m$ for ADP, facilitating an ability to act 'in reverse' as ATP-synthases [26]. This ATP-synthase activity was proposed to occur *in vivo* [26]. Thus, akin to Ins$P_5$ (inositol 1,3,4,5,6-pentakisphosphate) 2-kinase in plants [31], the IP6K reaction direction and rate of activity appear to be controlled by changes in ATP/ADP ratios [24]. These data have consolidated the idea that *PP*-Ins*P* turnover interfaces with cellular bioenergetic homoeostasis.

Experiments with partially purified native preparations of PPIP5K [25] have led to the conclusion that, just like IP6K, PPIP5K is reversible under *in vivo* conditions, such that cellular Ins$P_8$ levels can be controlled by physiological changes in ATP/ADP ratios [25]. This hypothesis has been well received [32–34]. However, it is a natural concern that the properties of partially purified native enzyme preparations may be influenced by contaminating proteins and other small-molecule modulators. The intrinsic lability of native PPIP5K [19] is also an issue. Thus, one of the goals of the current study was to use recombinant kinase to investigate through a kinetic study the manner in which PPIP5K activity – in both the 'forward' and 'reverse' directions – may be influenced by physiological changes in levels of adenine nucleotides as well as by the concentrations of inositol phosphate substrates.

Additionally, we should note that reliable data on reaction rates, reversibility and steady-state conditions are not the only parameters that systems biologists utilize when transferring kinetic data with isolated enzymes into mathematical models of metabolic pathways *in vivo*; information on reaction stoichiometry is also important [16]. In the current study we determined that PPIP5K's substrate-independent ATPase activity [20] is considerably more significant than was previously appreciated, and is stimulated up to 4-fold upon the binding of Ins*P* (inositol phosphate) substrate to the active site. We discuss the significance of this bioenergetic cost to the cell in terms of the roles of PPIPKs *in vivo*. We also discuss how this discovery of substrate-dependent ATPase activity of PPIP5K provided an opportunity to gain new insight into the reaction mechanism of this particular kinase.

One of the reasons that such extensive kinetic studies have not previously been performed with recombinant PPIP5Ks is the difficulties in obtaining samples of the *PP*-Ins*P*s with the appropriate degree of purity. *PP*-Ins*P*s are not commercially available and, at the time of writing, we are unaware of any laboratories that are currently chemically synthesizing these materials. *PP*-Ins*P*s can be prepared enzymatically but these highly charged molecules are inherently difficult to isolate in a salt-free form to a high degree of purity. Recently, a new method was introduced, which accomplishes that goal [35]. We have used these procedures in our study.

## MATERIALS AND METHODS

### Materials

Ins$P_6$ was purchased from Calbiochem and [$^3$H]Ins$P_6$ (~13.0 Ci/mmol) from PerkinElmer. Non-radiolabelled and [$^3$H]-radiolabelled *PP*-Ins*P*s (1-Ins$P_7$, 5-Ins$P_7$ and Ins$P_8$) were all synthesized enzymatically with the appropriate purified enzymes (see below). Deionized water was used throughout.

### Protein expression and purification

The human PPIP5K2 kinase domain (residues 1–366) [hPPIP5K2$^{KD}$, NCBI (National Center for Biotechnology Information) accession number NP_056031.2] and its single-site mutants were expressed in *Escherichia coli* and purified as previously described [20]. The protein was stored at −80 °C.

The human IP6K1 (NCBI accession number NP_695005.1) was expressed and purified as previously described for human PPIP5K1 and PPIP5K2 with the following modifications [18]: the protein was expressed with an N-terminal GST (glutathione transferase) tag in BL21 (DE3) *E. coli* (Stratagene) by induction overnight. Cells were sonicated in lysis buffer containing an EDTA-free complete protease inhibitor (Roche). The clarified lysate was loaded on to a 5 ml GSTrap HP (GE Healthcare) column, washed and eluted with a linear gradient from 0 to 30 mM of reduced glutathione in 25 mM Tris pH 8.0, 50 mM NaCl and 1 mM DTT (dithiothreitol). The protein was stored with 0.5 mg/ml BSA and 50% glycerol at −80 °C. The purity of our enzyme preparations were >95% (see Supplementary Figure S1 at http://www.bioscirep.org/bsr/033/bsr033e022add.htm).

### Preparation of *PP*-Ins*P*s

Enzymatic reactions were carried out in siliconized tubes (PGC Scientific) at 37 °C in 20 mM Hepes, pH 6.8, 50 mM NaCl, 6 mM $MgSO_4$, 1 mM DTT, 6 mM phosphocreatine, 24 unit/ml creatine kinase and 5 mM ATP disodium salt. Reactions (15 min) for the synthesis of [$^3$H]-radiolabelled 1-Ins$P_7$, 5-Ins$P_7$ and Ins$P_8$ contained 9.7 $\mu$Ci/ml [$^3$H]Ins$P_6$ (~13.0 Ci/mmol) and either, respectively, 0.076 mg/ml PPIP5K2$^{KD}$, 0.21 mg/ml GST–IP6K1 or 0.35 mg/ml GST–IP6K1 and 0.076 mg/ml PPIP5K2$^{KD}$. Reactions for the synthesis of non-radiolabelled 1-Ins$P_7$, 5-Ins$P_7$ and Ins$P_8$ contained 1.2 mM Ins$P_6$ and were conducted as follows, respectively: 0.12 mg/ml PPIP5K2$^{KD}$ for 22.5 h, 0.17 mg/ml GST–IP6K1 for 3 h or 0.17 mg/ml GST–IP6K1 and 0.11 mg/ml PPIP5K2$^{KD}$ for 3 h. Reactions were quenched and neutralized with, respectively, 0.2 volumes 2 M $HClO_4$ and 0.34 volumes

1 M $K_2CO_3$, 40 mM EDTA or placed at 100 °C for 3–5 min, then concentrated in a SpeedVac (Savant) at 43 °C to 300 $\mu$l.

The *PP*-Ins*P*s were then purified via a PAGE-based method [35] with the following modifications in order to scale up the procedure. Gels (31 cm×38.5 cm×1.5 mm) were run in a model S2 sequencing gel electrophoresis system (Life Technologies Gibco BRL) at 4 °C. Gels were prerun at 1000 V for 1 h prior to sample loading, then run at 1000 V for 48–60 h. The elution positions of the *PP*-Ins*P*s were determined in a 1 cm wide column at the edge of the gel. The non-radiolabelled *PP*-Ins*P*s were detected by staining with Toluidine Blue [35]. For the detection of *PP*-[$^3$H]Ins*P*s, the excised region of the gel was cut into 0.5 cm bands which were each mixed with 1 ml of Solusol (National Diagnostics) on a rocker (25 rev./min) for at least 5 h at room temperature, after which 4 ml of Soluscint XR (National Diagnostics) was added and samples were counted by liquid scintillation spectroscopy. To correct for any unevenness in the chromatography, the Orange-G dye front was used as a guide for determining the elution positions of the products (see Supplementary Figure S2 at http://www.bioscirep.org/bsr/033/bsr033e022add.htm). The appropriate sections of the gels were excised and washed with 5–10 ml 20 % (v/v) methanol, followed by a brief rinse with 5 ml water. The gel fragments were homogenized (Tekmar Tissuemizer Mark II) in 5 ml water at 20 500 rev./min at 0–4 °C prior to extraction of the *PP*-Ins*P*. Samples were concentrated to 1 ml (non-radiolabelled) or 4000 DPM/$\mu$l ([$^3$H]-radiolabelled) in a SpeedVac, aliquoted and stored at − 80 °C. No sample degradation was detected through a dozen freeze–thaw cycles over a period of several months.

Purity of *PP*-[$^3$H]Ins*P*s was assessed by HPLC (see the Results section). Non-radiolabelled *PP*-Ins*P*s were quantified by mass assay of the released orthophosphate upon complete hydrolysis by wet-ashing at 120 °C for 48 h [36,37].

## Enzyme assays

Kinetic parameters ($K_m$, $V_{max}$, $k_{cat}$ and $k_{cat}/K_m$) for adenine nucleotides and inositol phosphates were determined for PPIP5K2$^{KD}$ under pseudo first-order conditions [38]. Reactions (200 $\mu$l, 37 °C) simulating intracellular conditions contained 20 mM Hepes-NaOH pH 7.2, 50 mM KCl, 1 mg/ml bovine serum albumen, 1 mM EDTA disodium salt, 1 mM DTT, ATP or ADP disodium salt (1.1 $\mu$M to 10 mM), inositol phosphate (10 nM–10 $\mu$M), appropriate [$^3$H]-radiolabelled inositol phosphate tracer (4000 DPM) and PPIP5K2. Total $MgSO_4$ varied from 2 to 12 mM depending on ATP and ADP concentrations. Free $Mg^{2+}$ was 1.2 ± 0.1 mM (estimates performed with WebMaxc Extended, http://www.stanford.edu/~cpatton/webmaxc/webmaxcE.htm, last updated 7/3/09, accessed 8/24/11 [39]). Reactions were quenched and neutralized with, respectively, 0.2 volumes 2 M $HClO_4$ and 0.34 volumes 1 M $K_2CO_3$, 40 mM EDTA, then analysed by HPLC.

The mobile phase was initially run through a 4.6×250 mm silica presaturation column (Grace), before samples were loaded onto a 4.6×125 mm Partisphere 5 SAX column (Whatman). Buffer A was 1 mM EDTA disodium salt, Buffer B was 1.3 M $(NH_4)_2HPO_4$ (Sigma) plus 1 mM EDTA disodium salt, pH 3.85 with phosphoric acid (Aldrich). The gradient (1 ml/min) was as follows: 0–5 min, 0 % B; 5–10 min, B increased linearly from 0 to 45 %; 10–60 min, B increased linearly from 45 to 100 %; 60–75 min, B was 100 %. Each fraction (~30/assay, 1 ml each) was mixed with 4 ml MonoFlow 4 scintillant (National Diagnostics) and counted on a liquid scintillation counter for 10 min. For the kinetic determinations, assay linearity was confirmed under all conditions. The Michaelis–Menten equation was fit to plots of initial velocity against substrate concentration using non-linear regression to determine $K_m$ and $V_{max}$ values (GraphPad Prism v5.03). Results are presented as the means ± S.E.M. ($n \geqslant 2$). Similar assay conditions were used to determine equilibrium points.

## ATPase activity

ATPase activity (non-productive hydrolysis of ATP to ADP that did not drive phosphorylation of an Ins*P*) was determined by measurement of free orthophosphate in the reaction solution by the Malachite Green detection method used for quantification of *PP*-Ins*P* preparations (see above) 27–270 $\mu$g/ml PPIP5K2$^{KD}$ was incubated at 37 °C for 120 min in 50 $\mu$l reaction mixtures containing 20 mM Tris/HCl, pH 7.5, 10 mM ATP (unless otherwise indicated), 100 mM KCl, 0.1 mM EDTA and 5 mM $MgCl_2$. Results are presented as the means ± S.D. ($n = 3$).

## ATP synthesis by PPIP5K2$^{KD}$

The ATP synthase activity of PPIP5K2$^{KD}$ was determined in a 96-well microplate format by incubating 0.3 $\mu$g/ml enzyme at 37 °C for 15 min in 20 $\mu$l assays containing 1.4× reaction buffer (ATP Determination Kit, Molecular Probes), 650 $\mu$M ADP (ATP contamination < 1 ppm, Apollo Scientific Limited), 250 nM Ins$P_8$ and the indicated concentrations of either Ins$P_6$ or Ins$S_6$ (inositol hexasulphate). Then 16 $\mu$l of either an ATP standard solution or reaction solution was added into 100 $\mu$l Standard Reaction Solution (ATP Determination Kit, Molecular Probes) and luminescence was recorded after 15 s using a BioTek Synergy 2 microplate reader. The $IC_{50}$ values were determined using GraphPad Prism v5.03.

## Crystal structure determination

Crystals of PPIP5K2$^{KD}$ in complex with ADP were soaked with Ins$P_8$ using previously published procedures [20].

# RESULTS AND DISCUSSION

## Enzymatic synthesis and purity of *PP*-Ins*P*s

*PP*-Ins*P*s possess energetic phosphoanhydride bonds and undergo rapid turnover [27,28], so their cellular synthesis requires a considerable bioenergetic investment. Indeed, variations in cellular bioenergetic status have been proposed to influence *PP*-Ins*P* synthesis (see the Introduction section). We have investigated the role of PPIP5Ks in this process by determining the kinetic

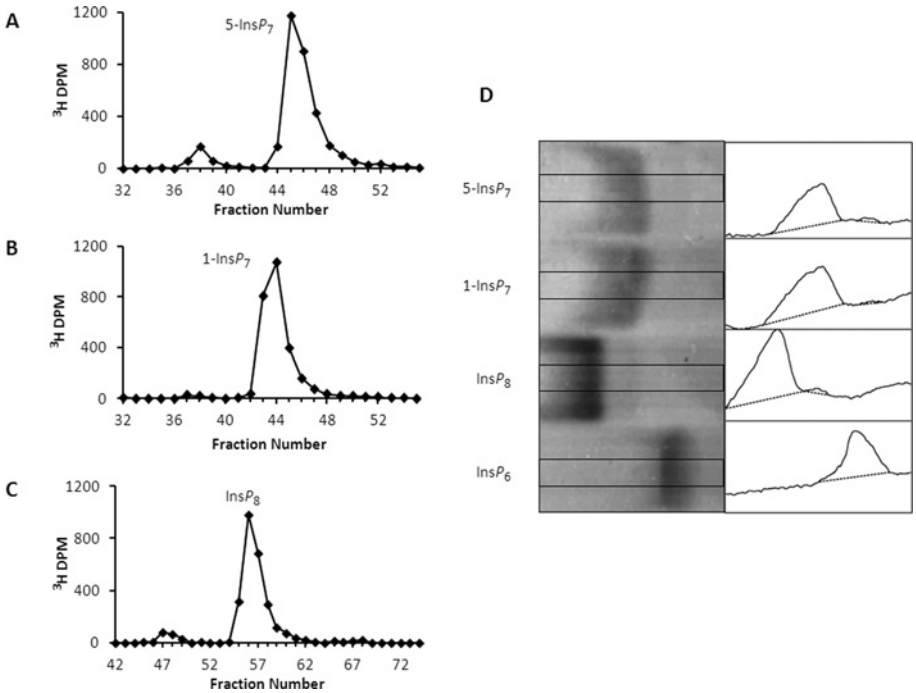


**Figure 2 Purity of *PP*-Ins*P* preparations**

HPLC (see the Materials and methods section) of 5-[$^3$H]Ins$P_7$ (**A**), 1-[$^3$H]Ins$P_7$ (**B**) and [$^3$H]Ins$P_8$ (**C**). The purities of 5-[$^3$H]Ins$P_7$, 1-[$^3$H]Ins$P_7$ and [$^3$H]Ins$P_8$ were 91, 98 and 92%, respectively. (**D**) Toluidine Blue-stained PAGE analysis (16 cm gel) of purity of non-radiolabelled *PP*-Ins*P* preparations (20 nmol/lane). The image was enhanced in ImageJ [54] by increasing contrast and smoothing. Purity was quantified by densitometric analysis (right-hand panels) of the central portion of each lane as indicated by the rectangles in each of the left-hand panels using ImageJ [54]. Commercial Ins$P_6$ (not further purified) served as a control. Purity was as follows: 5-Ins$P_7$, 96%; 1-Ins$P_7$, 98%; and Ins$P_8$, 97%.

properties of the kinase domain of recombinant human PPIP5K2 (PPIP5K2$^{KD}$).

One of our goals was to analyse the 'forward' (ATP-consuming) and 'reverse' (ATP-producing) reactions; that information has not previously been derived from recombinant enzyme. We therefore required three *PP*-Ins*P*s for this study, both radiolabelled and non-radiolabelled (1-Ins$P_7$, 5-Ins$P_7$ and Ins$P_8$; Figure 1). These *PP*-Ins*P*s were not commercially available, and to our knowledge there was not a laboratory that was chemically synthesizing these molecules. We therefore prepared them enzymatically, and purified them by a PAGE-based technique [35]. We determined that the purities of 5-[$^3$H]Ins$P_7$, 1-[$^3$H]Ins$P_7$ and [$^3$H]Ins$P_8$ were 91, 98 and 92%, respectively (Figures 2A–2C). The purities of 5-Ins$P_7$, 1-Ins$P_7$ and Ins$P_8$ were estimated to be 96, 98 and 97%, respectively (Figure 2D). This is an improvement over previous studies in which *PP*-Ins*P*s were either prepared enzymatically or chemically synthesized, whereupon the final products were 75–90% pure [18,19,40–42].

## Kinetic analysis of PPIP5K2$^{KD}$

We first used HPLC to analyse the PPIP5K-mediated phosphorylation of [$^3$H]-radiolabelled inositol phosphate substrates using saturating concentrations of ATP (see below) (Figures 3 and 4). Our data (Table 1) indicate that 5-Ins$P_7$ is the higher-affinity substrate; we found the $K_m$ value of PPIP5K2$^{KD}$ for Ins$P_6$ (0.4 $\mu$M; Table 1) to be 6.5-fold higher than that for 5-Ins$P_7$ (0.06 $\mu$M; Table 1). Our results are similar to the previously determined $K_m$ values for recombinant PPIP5Ks, 0.1 $\mu$M for Ins$P_6$ and 0.1–0.3 $\mu$M for 5-Ins$P_7$ [1,18,19]. These kinetic data demonstrate that the active site will be near-saturated by the levels of inositol phosphate substrates that occur *in vivo* [1,43]. However, one significant difference with earlier data is that we found that the $V_{max}$ values for these reactions (Table 1) were about 20–130-fold higher than those previously reported [18,19] for recombinant PPIP5K. This in turn is largely responsible for our values for $k_{cat}/K_m$ – the specificity constants – being up to 100-fold greater (Table 1) than that of previous determinations [18,19]. This brings the specificity constant for the PPIP5Ks much closer to that of the DIPPs (diphosphoinositol-polyphosphate phosphohydrolases) [44,45], and as such is more consistent with the long-standing observation that there is high ongoing turnover of *PP*-Ins*P*s *in vivo* [2,28]. Our much higher estimates for the $V_{max}$, which are likely due our obtaining correctly folded protein to a greater degree of purity, counter the argument that PPIP5K activity is too low to participate in 'phasic' signalling events [1].

Using saturating concentrations of either Ins$P_6$ or 5-Ins$P_7$, we next derived a substrate saturation plot for ATP; this showed

**Table 1 Kinetic parameters of PPIP5K2$^{KD}$:*PP*-Ins*P* synthesis**

Kinetic parameters were determined under pseudo first-order conditions [38] for phosphorylation of Ins$P_6$ or 5-Ins$P_7$ for both ATP and Ins*P* substrates (see the Materials and methods section). When fixed, ATP was 10 mM and Ins*P* 10 $\mu$M. Initial velocities were measured by conversion of an appropriate [$^3$H]-radiolabelled inositol phosphate tracer (4000 DPM) as analysed by Partisphere 5 SAX HPLC (e.g., see Figures 3A and 3C) for each data point. The Michaelis–Menten equation was fit to plots of initial velocity against substrate concentration using non-linear regression (GraphPad Prism v5.03). No substrate inhibition was observed (results not shown). Results are presented as the means ± S.E.M. ($n \geqslant 2$ independent experiments).

| | | $K_m$ ($\mu$M) | | | | $k_{cat}/K_m$ ($M^{-1} \cdot s^{-1}$) | |
|---|---|---|---|---|---|---|---|
| **Substrates** | | **Nucleotide** | **Ins*P*** | $V_{max}$ (nmol · min$^{-1}$ · mg$^{-1}$) | $k_{cat}$ ($s^{-1}$) | **Nucleotide** | **Ins*P*** |
| ATP | Ins$P_6$ | 37 ± 5 | 0.39 ± 0.09 | 43 ± 2 | 0.030 ± 0.001 | $7.9\times10^2$ | $7.6\times10^4$ |
| ATP | 5-Ins$P_7$ | 22 ± 7 | 0.060 ± 0.009 | 190 ± 10 | 0.13 ± 0.01 | $5.9\times10^3$ | $2.2\times10^6$ |

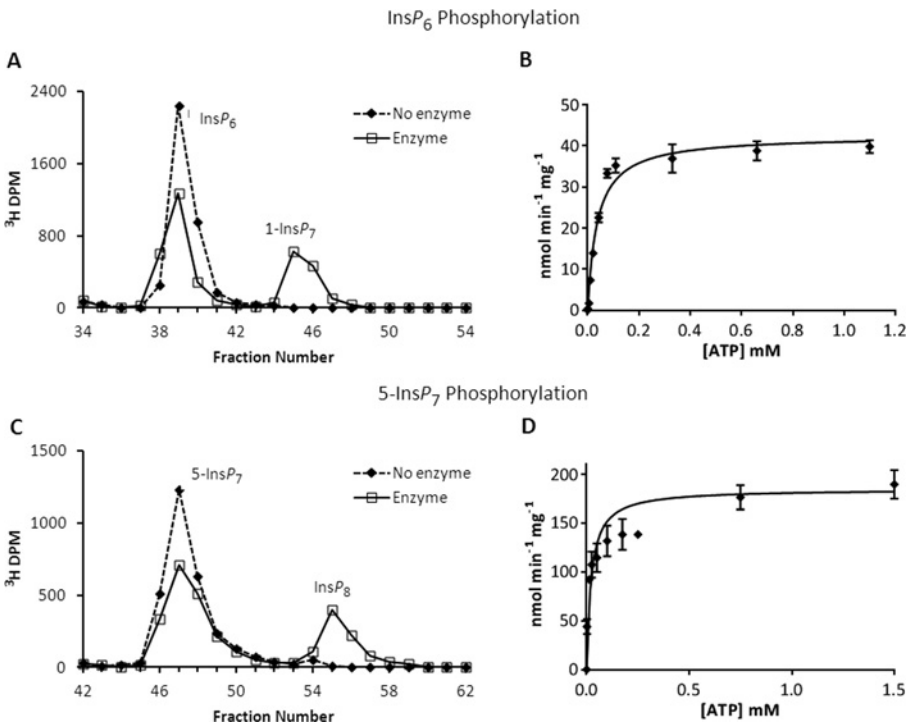


**Figure 3 Phosphorylation reactions of PPIP5K2$^{KD}$ and substrate saturation plots for ATP and ADP**

(**A**) Either no enzyme (broken line) or 27 $\mu$g/ml PPIP5K2$^{KD}$ (solid line) was incubated with 10 $\mu$M [$^3$H]Ins$P_6$, and 11 $\mu$M ATP for 20 min as indicated in the Materials and methods section. The reactions were quenched and neutralized and analysed by Partisphere SAX HPLC as described in the Materials and methods section. Representative HPLC data are shown. (**B**) The initial velocity of Ins$P_6$ phosphorylation was determined for forward reactions under pseudo first-order rate conditions [38] in which the concentration of the designated inositol phosphate was fixed at saturating levels (10 $\mu$M; Table 1), and the concentration of nucleotide was varied as indicated. Each individual data point was analysed by HPLC as described under the Materials and methods section. The Michaelis–Menten equation was fitted to the data using non-linear regression (GraphPad Prism v5.03). Results are presented as the means ± S.E.M. (**C**) Either no enzyme (broken line) or 0.011 $\mu$g/ml PPIP5K2$^{KD}$ (solid line) was incubated with 100 nM 5-[$^3$H]Ins$P_7$ and 10 mM ATP for 7 min as indicated in the Materials and methods section. The reactions were quenched and neutralized and analysed by Partisphere SAX HPLC as described in the Materials and methods section. Representative HPLC data are shown. (**D**) The initial velocity of 5-Ins$P_7$ phosphorylation was determined as described in the legend to panel (**B**) for Ins$P_6$.

Michaelis–Menten kinetics (Figures 3B and 3D). The value of the $K_m$ for ATP (22–37 $\mu$M; Table 1) was similar for both Ins$P_6$ and 5-Ins$P_7$. At an [ATP] of 1 mM, the $V_{max}$ values were already attained (Figures 3B and 3D); there was also no significant increase in reaction velocity when [ATP] was further increased to 10 mM (results not shown). These data lead us to conclude that *PP*-Ins*P* synthesis by PPIP5Ks is protected from physiologically relevant changes in [ATP] (1–5 mM [46]), contrary to the conclusion of a previous report [25]. As well as providing this new information about the characteristics of PPIP5Ks, our kinetic data (Table 1) can also be viewed as a successful quality control test of the recently developed PAGE-based procedures for purification of enzymatically prepared *PP*-Ins*P*s [35].

**Table 2 Kinetic parameters of PPIP5K2$^{KD}$:ATP synthesis**

Kinetic parameters were determined under pseudo first-order conditions [38] for dephosphorylation (ATP synthesis) of Ins$P_8$ or 1-Ins$P_7$ for both ADP and Ins*P* substrates (see the Materials and methods section). When fixed, ADP was 10 mM and Ins*P* 10 $\mu$M. Initial velocities were measured by conversion of an appropriate [$^3$H]-radiolabelled inositol phosphate tracer (4000 DPM) as analysed via Partisphere 5 SAX HPLC (e.g., see, Figures 4A and 4C) for each data point. The Michaelis–Menten equation was fit to plots of initial velocity against substrate concentration using non-linear regression (GraphPad Prism v5.03). No substrate inhibition was observed (results not shown). Results are presented as the means ± S.E.M. ($n \geqslant 2$ independent experiments).

| | | $K_m$ ($\mu$M) | | | | $k_{cat}/K_m$ ($M^{-1} \cdot s^{-1}$) | |
|---|---|---|---|---|---|---|---|
| **Substrates** | | **Nucleotide** | **Ins*P*** | $V_{max}$ (nmol · min$^{-1}$ · mg$^{-1}$) | $k_{cat}$ ($s^{-1}$) | **Nucleotide** | **Ins*P*** |
| ADP | Ins$P_8$ | 900 ± 280 | 0.022 ± 0.011 | 270 ± 30 | 0.19 ± 0.02 | $2.1\times10^2$ | $8.5\times10^6$ |
| ADP | 1-Ins$P_7$ | 5.2 ± 1.5 | 0.11 ± 0.01 | 2.8 ± 0.1 | 0.002 ± 0.000 | $3.7\times10^2$ | $1.7\times10^4$ |

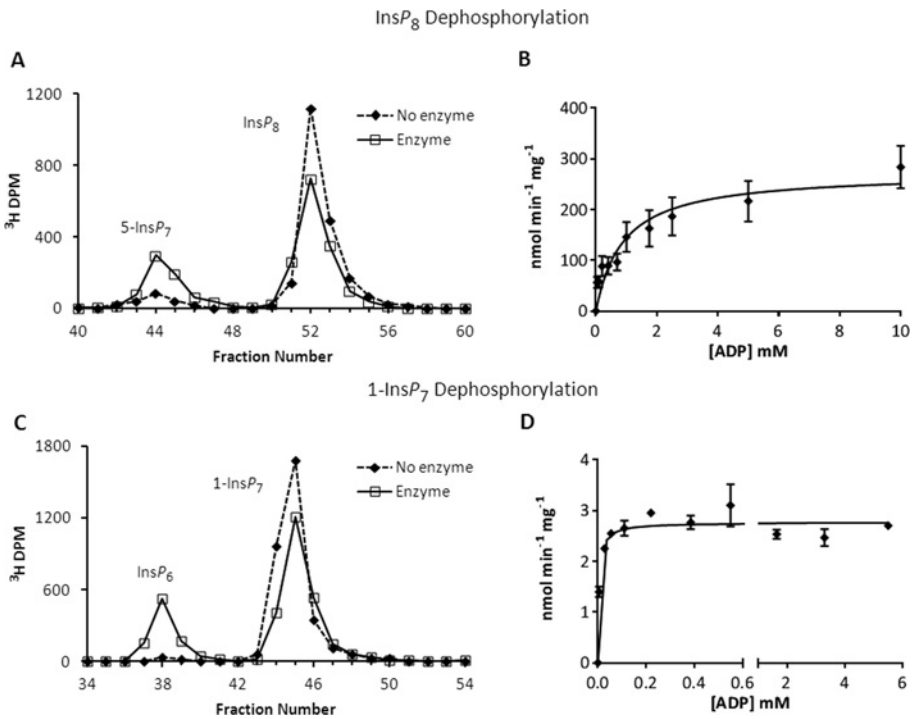


**Figure 4 Dephosphorylation reactions of PPIP5K2$^{KD}$ and substrate saturation plots for ATP and ADP**

(**A**) Either no enzyme (broken line) or 0.56 $\mu$g/ml PPIP5K2$^{KD}$ (solid line) was incubated with 10 $\mu$M [$^3$H]Ins$P_8$ and 5 mM ADP for 10 min as indicated in the Materials and methods section. The reactions were quenched and neutralized and analysed by Partisphere SAX HPLC as described in the Materials and methods section. Representative HPLC data are shown. (**B**) The initial velocity of Ins$P_8$ dephosphorylation was determined for reverse reactions under pseudo first-order rate conditions [38] in which the concentration of the designated inositol phosphate was fixed at saturating levels (10 $\mu$M; Table 1), and the concentration of nucleotide was varied as indicated. Each individual data point was analysed by HPLC as described under the Materials and methods section. The Michaelis–Menten equation was fitted to the data using non-linear regression (GraphPad Prism v5.03). Results are presented as the means ± S.E.M. (**C**) Either no enzyme (broken line) or 27 $\mu$g/ml PPIP5K2$^{KD}$ (solid line) was incubated with 10 $\mu$M 1-[$^3$H]Ins$P_7$ and 28 $\mu$M ADP for 45 min as indicated in the Materials and methods section. The reactions were quenched and neutralized and analysed by Partisphere SAX HPLC as described in the Materials and methods section. Representative HPLC data are shown. (**D**) The initial velocity of 1-Ins$P_7$ dephosphorylation was determined as described in the legend to panel (**B**) for Ins$P_8$.

## Reversibility of PPIP5K and the consequences of substrate competition

Several inositol phosphate kinases have been shown to be physiologically reversible, that is, their relative rates of phosphorylation and dephosphorylation can be influenced by changes in cellular [ATP]/[ADP] ratios: IP6K [26], Ins$P_5$ 2-kinase [31] and ITPK1 (inositol 1,3,4-trisphosphate 5/6-kinase) [47]. A previous report [25] has included the PPIP5Ks in this category. The degree of the ATP-synthase activities of IP6Ks and PPIP5Ks were further proposed [25,26] to be regulated by physiological changes in adenine nucleotide levels. This idea, which dovetails with the concept that *PP*-Ins*P*s are highly energetic phosphate donors [26,27], has become well accepted in the field [32–34,48].

We found that PPIP5K2$^{KD}$ was reversible *in vitro* when it was incubated with ADP plus either 1-Ins$P_7$ or Ins$P_8$ (Figure 4). Substrate saturation curves showed the reactions to follow Michaelis–Menten kinetics (Figures 4B and 4D). The

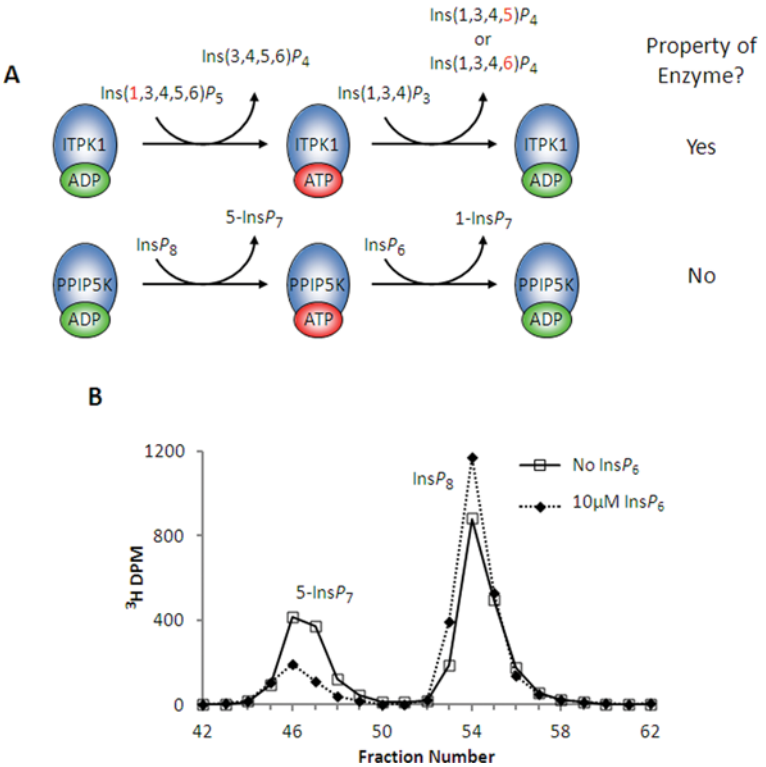


**Figure 5** **PPIP5K2$^{KD}$ is not a phosphotransferase: Ins$P_6$ inhibits Ins$P_8$ dephosphorylation by PPIP5K2$^{KD}$**

(**A**, top) This graphic depicts how Ins(1,3,4)$P_3$ stimulates Ins(1,3,4,5,6)$P_5$ dephosphorylation by ITPK1 [47]. The 1-phosphate group (shown in red) that is removed from Ins(1,3,4,5,6)$P_5$ is not released into the bulk phase but is retained by the nucleotide and donated to Ins(1,3,4)$P_3$; this returns the enzyme to its ADP state, ready for another cycle of Ins(1,3,4,5,6)$P_5$ dephosphorylation. (**A**, bottom) The analogous potential reaction sequence for PPIP5K. (**B**) Either no enzyme (broken line) or 0.63 $\mu$g/ml PPIP5K2$^{KD}$ (solid line; dotted line) was incubated with 10 $\mu$M [$^3$H]Ins$P_8$ and 10 mM ADP for 10 min as indicated in the Materials and methods section. Where indicated (dotted line) incubations also contained 10 $\mu$M Ins$P_6$. The reactions were quenched and neutralized and analysed by Partisphere SAX HPLC as described in the Materials and methods section. Representative HPLC data are shown.

dephosphorylation of Ins$P_8$ proceeded at a slightly greater $V_{max}$ (Tables 1 and 2) than did the corresponding forward reaction (5-Ins$P_7$ phosphorylation). For the dephosphorylation of Ins$P_8$ the $K_m$ for ADP was 0.9 mM (Table 2), which is within the range of physiological total ADP concentrations (0.7–1.7 mM; [46]). Interestingly, for the dephosphorylation of 1-Ins$P_7$, the value for the $K_m$ of ADP was 175-fold lower, and thus much closer to the $K_m$ values for ATP in the phosphorylation reactions (Table 2).

The high rate of dephosphorylation of Ins$P_8$ by PPIP5K2$^{KD}$ was somewhat surprising in view of our earlier structural data [20] which indicated that, in the crystal complex of PPIP5K2$^{KD}$, the Ins$P_8$ product was under considerable steric strain. It had seemed reasonable to conclude that the increase in entropy upon product release would discourage re-binding of Ins$P_8$ for dephosphorylation. Thus, we soaked Ins$P_8$ into a crystal complex of PPIP5K2$^{KD}$ and ADP. We found the conformation and catalytic environments of this complex to be very similar (results not shown) to those that we described previously when Ins$P_8$ was synthesized inside the crystals [20]. We therefore have no evidence that the mechanism of Ins$P_8$ dephosphorylation proceeds any differently than by a reversal of 5-Ins$P_7$ phosphorylation.

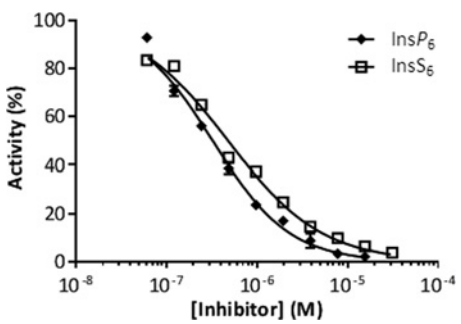


**Figure 6** **Ins$P_6$ and Ins$S_6$ inhibit Ins$P_8$ dephosphorylation by PPIP5K2$^{KD}$; a luciferase-based ATP assay**

A total of 0.3 $\mu$g/ml PPIP5K2$^{KD}$ was incubated at 37 °C with 1.4× reaction buffer (ATP Determination Kit, Molecular Probes), 650 $\mu$M ADP and 250 nM Ins$P_8$ for 15 min as described in the Materials and methods section. Ins$S_6$ and Ins$P_6$ were included in the assays as indicated. Then 16 $\mu$l of either an ATP standard solution or reaction solution was added into 100 $\mu$l Standard Reaction Solution (ATP Determination Kit, Molecular Probes) and luminescence was recorded after 15 s using a BioTek Synergy 2. Data are presented as the means ± S.E.M. ($n \geqslant 3$). A dose–response curve was fit using GraphPad Prism v5.03. The $IC_{50}$ values for Ins$S_6$ and Ins$P_6$ were 0.48 and 0.32 $\mu$M, respectively.

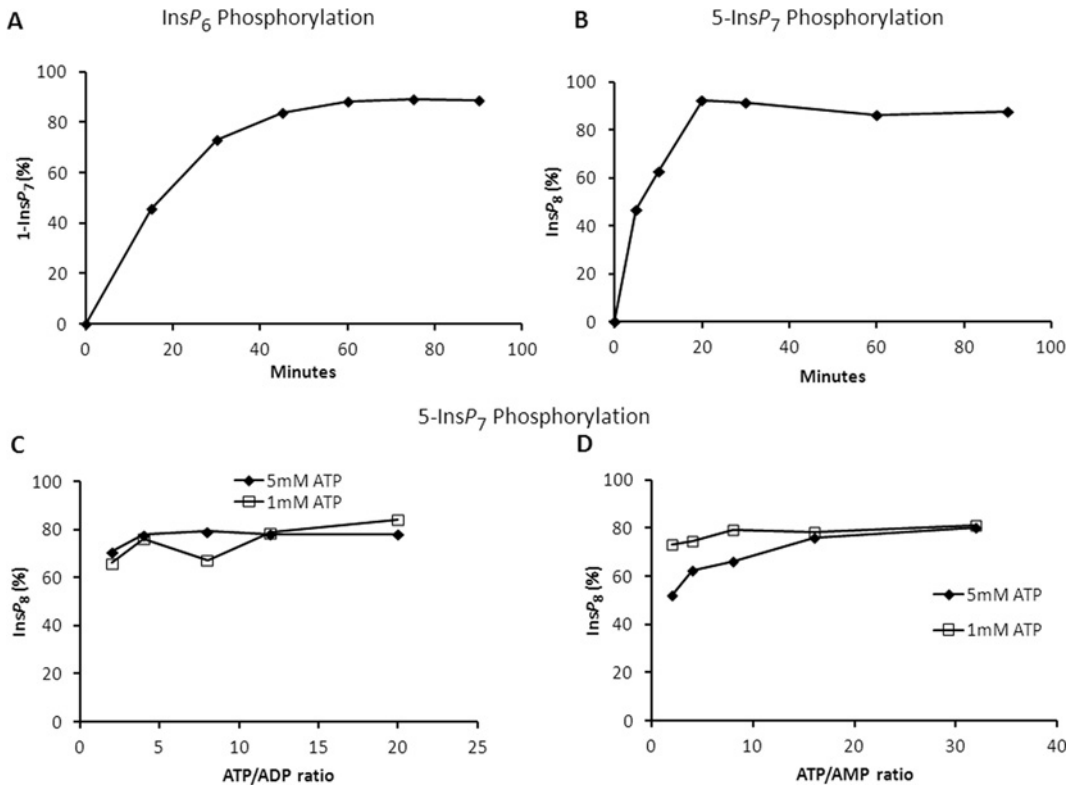


**Figure 7** **Effect of ATP/ADP and AMP upon the equilibrium condition for PPIP5K2$^{KD}$**

(**A**) and (**B**) show a time course of Ins$P_6$ and 5-Ins$P_7$ phosphorylation, respectively. In (**A**), 20 $\mu$g/ml enzyme was incubated with reaction buffer (see the Materials and methods section) containing 15 $\mu$M Ins$P_6$, 5 mM ATP and 0.5 mM ADP. In (**B**), 0.33 $\mu$g/ml enzyme was incubated with reaction buffer (see the Materials and methods section) containing 1 $\mu$M 5-Ins$P_7$ and 5 mM ATP. Assays were quenched and neutralized and analysed by Partisphere SAX HPLC as described in the Materials and methods section. (**C**) and (**D**) show the equilibrium point for the phosphorylation of 5-Ins$P_7$ to Ins$P_8$ in which 0.33 $\mu$g/ml enzyme was incubated as described in the Materials and methods section under initial conditions of 1 $\mu$M 5-Ins$P_7$ and either 1 (squares) or 5 (diamonds) mM ATP; either the ATP/ADP ratio (**C**) or the ATP/AMP ratio (**D**) was varied as indicated. Assays were conducted for 60 min. The reactions were then quenched and neutralized and analysed by Partisphere SAX HPLC as described in the Materials and methods section.

One of the other inositol phosphate kinases that is reversible, ITPK1, is PPIP5K's closest structural homologue [20]. Both PPIP5K2 and ITPK1 envelop ATP tightly within two sets of antiparallel $\beta$-sheets that comprise an ATP-grasp fold; in each case, less than 10% of the nucleotide is solvent exposed [20,47]. In the case of ITPK1, the bound nucleotide promotes a phosphotransferase activity by which the dephosphorylation of Ins(1,3,4,5,6)$P_5$ to Ins(3,4,5,6)$P_4$ is stimulated by the phosphorylation of Ins(1,3,4)$P_3$ [47]. The analogous reaction for PPIP5K would be the stimulation of Ins$P_8$ dephosphorylation by the presence of Ins$P_6$ (Figure 5A). To investigate if that were possible, we assayed the 'reverse' (i.e., Ins$P_8$ dephosphorylation) activity of PPIP5K2$^{KD}$ in the presence of physiological [Ins$P_6$] (Figure 5B). Unlike ITPK1, the phosphorylation of one substrate (Ins$P_6$) by PPIP5K2$^{KD}$ merely inhibited (by >70%) the dephosphorylation of another (Ins$P_8$) (Figure 5B). We conclude that even though both ITPK1 and PPIP5K are ATP-grasp kinases, only ITPK1 can act as a phosphotransferase.

The inhibition of Ins$P_8$ dephosphorylation by Ins$P_6$ was also demonstrated by using a luciferase-based ATP-detection method ($IC_{50} = 0.32$ $\mu$M; Figure 6). The latter result indicates that the luciferase assay could be employed as a high-throughput tool to screen for inhibitors of this enzyme. For example, by using this method we found that Ins$S_6$ also inhibited the enzyme ($IC_{50} = 0.48$ $\mu$M; Figure 6).

## Equilibrium and rate studies of PPIP5K2$^{KD}$ under varied [ATP] and [ADP]

Tables 1 and 2 show that PPIP5K2$^{KD}$ is reversible *in vitro* and also Ins$P_8$ dephosphorylation was associated with a $K_m$ value for ADP that has potential physiological relevance. We therefore next investigated to what extent changes in the initial ATP/ADP ratios would influence either the initial reaction rate or equilibrium point of the kinase reaction.

In planning these experiments, we noted that total cellular [ATP] generally varies between 1 and 5 mM, with total cellular ATP/ADP ratios generally in the range of 2–12 [46,49,50]. At physiologically relevant [ATP] and [ADP] concentrations of 5 and 0.5 mM, respectively, the PPIP5K2$^{KD}$-catalysed

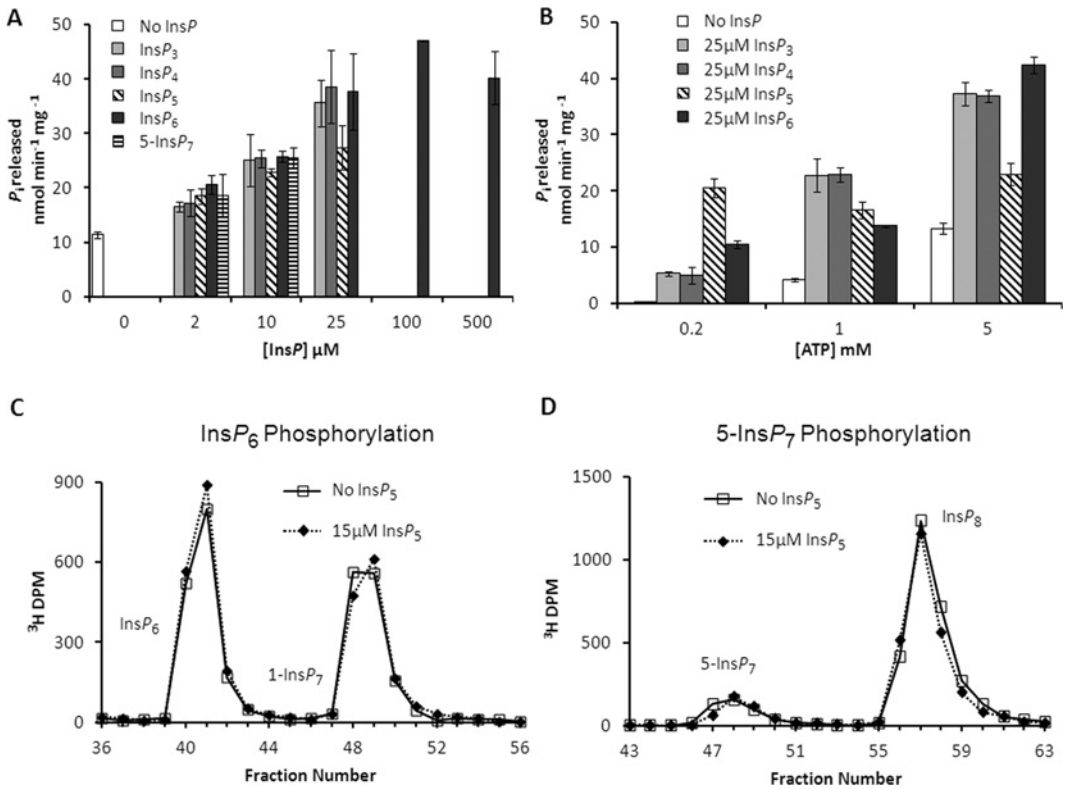


**Figure 8 ATPase activity of PPIP5K2$^{KD}$**

(**A**) and (**B**) *Ortho*phosphate released from the hydrolysis of ATP was measured using a Malachite Green detection method [55]. The 27–270 $\mu$g/ml PPIP5K2$^{KD}$ was incubated at 37 °C for 120 min in 50 $\mu$l reactions containing 20 mM Tris/HCl, pH 7.5, 10 mM ATP (unless otherwise indicated), 100 mM KCl, 0.1 mM EDTA and 5 mM $MgCl_2$. (**A**) Stimulation of PPIP5K2$^{KD}$ ATPase activity by Ins$P_3$, Ins$P_4$, Ins$P_5$, Ins$P_6$ and 5-Ins$P_7$ (concentrations as indicated, [ATP] = 5 mM). (**B**) Effect of ATP concentration (0.2, 1 or 5 mM) on basal (absence of Ins*P*) and Ins*P*-stimulated (25 $\mu$M) ATPase activity. Results are presented as the means ± S.D. ($n = 3$). (**C**) and (**D**) provide representative HPLC data indicating that 15 $\mu$M Ins$P_5$ (dotted lines) does not inhibit phosphorylation of either Ins$P_6$ or 5- Ins$P_7$, respectively. In (**C**), 20 $\mu$g/ml PPIP5K2$^{KD}$ was incubated for 15 min with reaction buffer (see the Materials and methods section) containing 15 $\mu$M [$^3$H]Ins$P_6$, 5 mM ATP and 0.5 mM ADP. In (**D**), 0.41 $\mu$g/ml PPIP5K2$^{KD}$ was incubated for 5 min with reaction buffer (see the Materials and methods section) containing 1 $\mu$M 5-[$^3$H]Ins$P_7$, 5 mM ATP and 0.5 mM ADP. The reactions were quenched and neutralized and analysed by Partisphere SAX HPLC as described in the Materials and methods section.

equilibrium point was attained at near complete (80–90 %) phosphorylation of either Ins$P_6$ or 5-Ins$P_7$ (Figures 7A–7C). Furthermore, the PPIP5K equilibrium point for the phosphorylation of 5-Ins$P_7$ to Ins$P_8$ was neither affected by varying total ATP (1 or 5 mM) nor by changing the ATP/ADP ratio from 2 to 20 (Figure 7C). We also assayed PPIP5K2$^{KD}$ activity under physiological extremes of ATP/ADP ratio (2 against 20), using both 1 and 5 mM total [ATP] (results not shown). The changes that we made to the ATP/ADP ratios did not alter reaction rates. These data indicate that the reversibility of PPIP5Ks is not biologically significant *in vivo*, in contrast to a previous proposal [25]. Although the $V_{max}$ for Ins$P_8$ dephosphorylation is relatively high, the enzyme's relatively low affinity for ADP may in part explain why that reaction is not favoured, as long as physiological levels of ATP are also present. Our data also demonstrate that the synthesis of both 1-Ins$P_7$ and Ins$P_8$ is likely well-protected from the consequences of the deteriorating [ATP]/[ADP] ratio that cells experience when undergoing bioenergetic stress.

## Equilibrium and rate studies of PPIP5K2$^{KD}$ under varied [AMP]

Ins$P_8$ levels *in vivo* have been found to decrease in response to mild bioenergetic stress that is reflected more in an increase in [AMP] rather than a decrease in [ATP]/[ADP] [15]. However, we did not find any effect of AMP upon the equilibrium condition catalysed by PPIP5K2$^{KD}$ (Figure 7D). We further found that these same changes in [ATP]/[AMP] ratios did not affect PPIP5K2$^{KD}$ reaction rate (results not shown). Thus the decrease in Ins$P_8$ in relation to elevated [AMP] *in vivo* [15] likely proceeds through a signalling pathway, rather than through direct effects on Ins$P_8$ synthesis by PPIP5K2. We [15] have previously excluded AMPK (AMP-activated protein kinase) from being involved, so we will need to consider other mechanisms.

## The stoichiometry of PPIP5K2$^{KD}$

Reaction stoichiometry is pertinent to the regulation of metabolic pathways [16]. Moreover, since PPIP5K activity consumes ATP, stoichiometry is also highly relevant to the potential interface of

*PP*-Ins*P*s with cellular bioenergetic status [5,15]. We [20] previously demonstrated that PPIP5K2 showed a slow ATPase activity (0.5 nmol $min^{-1}$ $mg^{-1}$) when it was incubated with 0.1 mM ATP in the absence of inositol phosphate substrate. That did not seem significant in relation to the $V_{max}$ values for Ins$P_6$ and 5-Ins$P_7$ phosphorylation (43 and 190 nmol $min^{-1}$ $mg^{-1}$; Table 1). However, in the current study we found that at physiological [ATP] (5 mM), the inositol phosphate-independent ATPase activity increased to approximately 12 nmol $min^{-1}$ $mg^{-1}$ (Figures 8A and 8B). Moreover, the rate of ATP hydrolysis was further elevated up to 4-fold as increasing concentrations of either Ins$P_6$ or 5-Ins$P_7$ were added, with a maximally effective concentration of 25 $\mu$M (Figure 8A).

Ins$P_3$ (inositol 1,3,4-trisphosphate), Ins$P_4$ (inositol 1,3,4,5-tetrakisphosphate) and Ins$P_5$ also stimulated ATPase activity (Figures 8A and 8B). These Ins*P*s elevated ATPase activity even at low (0.2 $\mu$M) [ATP] (Figure 8B). It is surprising that this ATPase activity can be stimulated by an inositol phosphate that is neither a substrate [20] nor an inhibitor (Figures 8C and 8D). Nevertheless, such data (Figures 8C and 8D) lead us to conclude that even the relatively high levels of Ins$P_5$ that occur in cells cannot access the enzyme's active site to stimulate ATPase activity when Ins$P_6$ and 5-Ins$P_7$ are available.

A comparison of the rates of the ATPase activity (Figures 8A and 8B) in relation to the kinase activity (Table 1) indicates that approximately two molecules of ATP are consumed for every molecule of Ins$P_6$ that is phosphorylated. As the $V_{max}$ is higher for 5-Ins$P_7$ phosphorylation compared with Ins$P_6$ phosphorylation (Table 1), there is a much smaller impact of the ATPase activity upon that reaction stoichiometry (1.2 molecules of ATP are consumed for every molecule of 5-Ins$P_7$ that is phosphorylated). In other words, the bioenergetic cost to the cell is much smaller for 5-Ins$P_7$ phosphorylation (17% ATP 'wastage') than it is for Ins$P_6$ phosphorylation (50% ATP 'wastage'). Thus, the synthesis of Ins$P_8$ by pathway I is more energetically efficient than is pathway II (Figure 1).

An analogous ATPase reaction has been observed in ATP-grasp ligases [51], but to our knowledge this is the first demonstration that this is a property of an ATP-grasp kinase. We propose that the dynamic nature of the active site and the partly associative reaction mechanism make it inevitable that there will be some non-productive ATPase activity. We [20] have also previously determined that Ins$P_6$ is more mobile within the active site than is 5-Ins$P_7$. That may explain why the phosphorylation of Ins$P_6$ is less efficient.

We studied the mechanism of this ATPase activity through structural and mutagenesis studies. Previous analysis [20] of the crystal structure of the PPIP5K2$^{KD}$ indicated that there are two water molecules (W1 and W2; Figure 9A) that are candidates to carry out nucleophilic attack on the $\gamma$-phosphate of ATP (Figure 9A). The two amino acid residues that are candidates for activating these putative nucleophiles are $Arg^{213}$ and $Lys^{248}$, respectively (Figure 9A). We therefore assayed ATPase activities of R213A and K248A mutants of PPIP5K2$^{KD}$. Both mutants showed a reduction in Ins$P_6$-stimulated ATPase activity, as expected since $Arg^{213}$ and $Lys^{248}$ are required for binding of Ins$P_6$ [20]. In contrast, only the K248A mutant showed a significant reduction in the rate of inositol phosphate-independent ATPase activity (Figure 9B). We therefore conclude that W2 is the water molecule that is activated for nucleophilic attack upon the $\gamma$-phosphate of ATP.

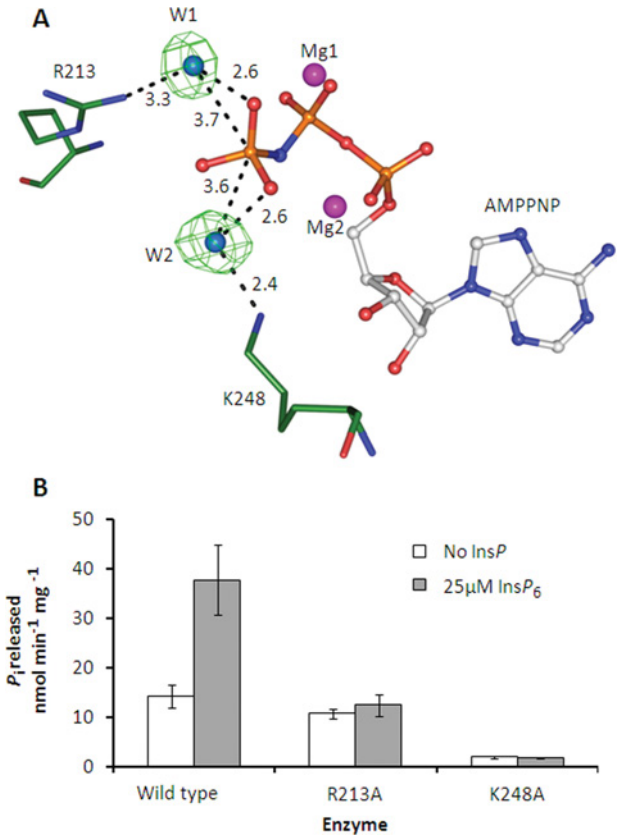


**Figure 9 The effects of R213A and K248A mutations upon ATPase activity of PPIP5K2$^{KD}$**

(**A**) Structure of a portion of the wild-type PPIP5K2$^{KD}$ catalytic centre [20] showing water molecules bridging the interaction between the ATP analogue AMPPNP (adenosine 5′-[$\beta$,$\gamma$-imido]triphosphate) and R213 and K248. (**B**) The effect of single-site mutants of PPIP5K2$^{KD}$ on basal and Ins$P_6$-stimulated (25 $\mu$M) ATPase activity. ATPase activity was measured as in Figure 8.

## CONCLUDING COMMENTS

Our new kinetic information concerning PPIP5K stoichiometry, rates, substrate affinities and equilibrium conditions assists our understanding of the dynamic behaviour of this signalling enzyme *in vivo* and the role it has in *PP*-Ins*P* generation. Since the catalytic and structural features of the active sites of PPIP5K1 and PPIP5K2 are so similar [18,20], we believe the conclusions that we have made are equally applicable to both enzymes. Furthermore, our studies with recombinant protein have led us to conclude that contrary to an earlier report [25], the kinetic characteristics of PPIP5Ks do not match the synthesis of Ins$P_8$ to

fluctuations in adenine nucleotide levels. Instead, the opposite is true; the kinetic properties of PPIP5Ks ensure that Ins$P_8$ synthesis is protected against cellular bioenergetic stress. The features of this enzyme stand in contradiction to the reduction in Ins$P_8$ levels that accompanies experimental manipulations in cultured cells that are generally thought to invoke mild bioenergetic stress [15]. It will be important to uncover the signalling pathways that are involved and their biological relevance.

## AUTHOR CONTRIBUTION

Jeremy Weaver, Huanchen Wang and Stephen Shears designed the experiments, analysed the results and wrote the paper. Jeremy Weaver and Huanchen Wang conducted the experiments.

## FUNDING

This work was supported by the Intramural Research Program of the National Institutes of Health/National Institute of Environmental Health Sciences.

## REFERENCES

1 Wundenberg, T. and Mayr, G. W. (2012) Synthesis and biological actions of diphosphoinositol phosphates (inositol pyrophosphates), regulators of cell homeostasis. Biol. Chem. **393**, 979–998
2 Saiardi, A. (2012) Cell signalling by inositol pyrophosphates. Subcell. Biochem. **59**, 413–443
3 Chakraborty, A., Kim, S. and Snyder, S. H. (2011) Inositol pyrophosphates as mammalian cell signals. Sci. Signaling **4**, re1
4 Tsui, M. M. and York, J. D. (2010) Roles of inositol phosphates and inositol pyrophosphates in development, cell signaling and nuclear processes. Adv. Enzyme Regul. **50**, 324–337
5 Shears, S. B. (2009) Diphosphoinositol polyphosphates: metabolic messengers? Mol. Pharmacol. **76**, 236–252
6 Barker, C. J., Illies, C., Gaboardi, G. C. and Berggren, P. O. (2009) Inositol pyrophosphates: structure, enzymology and function. Cell. Mol. Life Sci. **66**, 3851–3871
7 Lee, Y. S., Mulugu, S., York, J. D. and O'Shea, E. K. (2007) Regulation of a cyclin-cdk-cdk inhibitor complex by inositol pyrophosphates. Science **316**, 109–112
8 Chakraborty, A., Koldobskiy, M. A., Bello, N. T., Maxwell, M., Potter, J. J., Juluri, K. R., Maag, D., Kim, S., Huang, A. S., Dailey, M. J. et al. (2010) Inositol pyrophosphates inhibit Akt signaling, thereby regulating insulin sensitivity and weight gain. Cell **143**, 897–910
9 Azevedo, C., Burton, A., Ruiz-Mateos, E., Marsh, M. and Saiardi, A. (2009) Inositol pyrophosphate mediated pyrophosphorylation of AP3B1 regulates HIV-1 Gag release. Proc. Natl. Acad. Sci. U.S.A. **106**, 21161–21166
10 Bhandari, R., Saiardi, A., Ahmadibeni, Y., Snowman, A. M., Adam, R. C., Kristiansen, T. Z., Molina, H., Pandey, A., Werner, J. K., Jr, Juluri, K. R. et al. (2007) Protein pyrophosphorylation by inositol pyrophosphates is a posttranslational event. Proc. Natl. Acad. Sci. U.S.A. **104**, 15305–15310
11 Saiardi, A., Bhandari, R., Resnick, A. C., Snowman, A. M. and Snyder, S. H. (2004) Phosphorylation of proteins by inositol pyrophosphates. Science **306**, 2101–2105
12 Choi, K., Mollapour, E. and Shears, S. B. (2005) Signal transduction during environmental stress: InsP8 operates within highly restricted contexts. Cell Signal. **17**, 1533–1541
13 Pesesse, X., Choi, K., Zhang, T. and Shears, S. B. (2004) Signaling by higher inositol polyphosphates: synthesis of bisdiphosphoinositol tetrakisphosphate ('InsP8') is selectively activated by hyperosmotic stress. J. Biol. Chem. **279**, 43378–43381
14 Onnebo, S. M. N. and Saiardi, A. (2009) Inositol pyrophosphates modulate hydrogen peroxide signalling. Biochem. J. **423**, 109–118
15 Choi, K., Mollapour, E., Choi, J. H. and Shears, S. B. (2008) Cellular energetic status supervises the synthesis of bis-diphosphoinositol tetrakisphosphate independently of AMP-activated protein kinase. Mol. Pharmacol. **74**, 527–536
16 Rohwer, J. M. (2012) Kinetic modelling of plant metabolic pathways. J. Exp. Bot. **63**, 2275–2292
17 Padmanabhan, U., Dollins, D. E., Fridy, P. C., York, J. D. and Downes, C. P. (2009) Characterization of a selective inhibitor of inositol hexakisphosphate kinases. Use in defining biological roles and metabolic relationships of inositol pyrophosphates. J. Biol. Chem. **284**, 10571–10582
18 Fridy, P. C., Otto, J. C., Dollins, D. E. and York, J. D. (2007) Cloning and characterization of two human VIP1-like inositol hexakisphosphate and diphosphoinositol pentakisphosphate kinases. J. Biol. Chem. **282**, 30754–30762
19 Choi, J. H., Williams, J., Cho, J., Falck, J. R. and Shears, S. B. (2007) Purification, sequencing, and molecular identification of a mammalian PP-InsP5 kinase that is activated when cells are exposed to hyperosmotic stress. J. Biol. Chem. **282**, 30763–30775
20 Wang, H., Falck, J. R., Hall, T. M. T. and Shears, S. B. (2012) Structural basis for an inositol pyrophosphate kinase surmounting phosphate crowding. Nat. Chem. Biol. **8**, 111–116
21 Mulugu, S., Bai, W., Fridy, P. C., Bastidas, R. J., Otto, J. C., Dollins, D. E., Haystead, T. A., Ribeiro, A. A. and York, J. D. (2007) A conserved family of enzymes that phosphorylate inositol hexakisphosphate. Science **316**, 106–109
22 Gokhale, N. A., Zaremba, A. and Shears, S. B. (2011) Receptor-dependent compartmentalization of PPIP5K1, a kinase with a cryptic polyphosphoinositide binding domain. Biochem. J. **434**, 415–426
23 Szijgyarto, Z., Garedew, A., Azevedo, C. and Saiardi, A. (2011) Influence of inositol pyrophosphates on cellular energy dynamics. Science **334**, 802–805
24 Nagel, A., Barker, C. J., Berggren, P. O. and Illies, C. (2010) Diphosphosinositol polyphosphates and energy metabolism: assay for ATP/ADP ratio. Methods Mol. Biol. **645**, 123–131
25 Huang, C. F., Voglmaier, S. M., Bembenek, M. E., Saiardi, A. and Snyder, S. H. (1998) Identification and purification of diphosphoinositol pentakisphosphate kinase, which synthesizes the inositol pyrophosphate bis(diphospho)inositol tetrakisphosphate. Biochemistry **37**, 14998–15004
26 Voglmaier, S. M., Bembenek, M. E., Kaplin, A. I., Dormán, G., Olszewski, J. D., Prestwich, G. D. and Snyder, S. H. (1996) Purified inositol hexakisphosphate kinase is an ATP synthase: diphosphoinositol pentakisphosphate as a high-energy phosphate donor. Proc. Natl. Acad. Sci. U.S.A. **93**, 4305–4310
27 Stephens, L., Radenberg, T., Thiel, U., Vogel, G., Khoo, K. H., Dell, A., Jackson, T. R., Hawkins, P. T. and Mayr, G. W. (1993) The detection, purification, structural characterization, and metabolism of diphosphoinositol pentakisphosphate(s) and bisdiphosphoinositol tetrakisphosphate(s). J. Biol. Chem. **268**, 4009–4015
28 Menniti, F. S., Miller, R. N., Putney, Jr, J. W. and Shears, S. B. (1993) Turnover of inositol polyphosphate pyrophosphates in pancreatoma cells. J. Biol. Chem. **268**, 3850–3856
29 Knight, Z. A. and Shokat, K. M. (2005) Features of selective kinase inhibitors. Chem. Biol. **12**, 621–637
30 Shears, S. B. (2004) How versatile are inositol phosphate kinases? Biochem. J. **377**, 265–280

31 Phillippy, B. Q., Ullah, A. H. and Ehrlich, K. C. (1994) Purification and some properties of inositol 1,3,4,5,6-pentakisphosphate 2-kinase from immature soybean seeds. J. Biol. Chem. **269**, 28393–28399
32 Raboy, V. (2009) Approaches and challenges to engineering seed phytate and total phosphorus. Plant Sci. **177**, 281–296
33 Losito, O., Szijgyarto, Z., Resnick, A. C. and Saiardi, A. (2009) Inositol pyrophosphates and their unique metabolic complexity: analysis by gel electrophoresis. PLoS ONE **4**, e5580
34 Fisher, S. K., Novak, J. E. and Agranoff, B. W. (2002) Inositol and higher inositol phosphates in neural tissues: homeostasis, metabolism and functional significance. J. Neurochem. **82**, 736–754
35 Loss, O., Azevedo, C., Szijgyarto, Z., Bosch, D. and Saiardi, A. (2011) Preparation of quality inositol pyrophosphates. J. Vis. Exp. **55**, e3027
36 Perelló, J., Isern, B., Muñoz, J. A., Valiente, M. and Grases, F. (2004) Determination of phytate in urine by high-performance liquid chromatography-mass spectrometry. Chromatographia **60**, 265–268
37 Hoenig, M., Lee, R. J. and Ferguson, D. C. (1989) A microtiter plate assay for inorganic-phosphate. J. Biochem. Biophys. Methods **19**, 249–251
38 Brooks, H. B., Geeganage, S., Kahl, S. D., Montrose, C., Sittampalam, S., Smith, M. C. and Weidner, J. R. (2004) Basics of enzymatic assays for HTS. In Assay Guidance Manual (Sittampalam, G. S., Weidner, J., Auld, D., Glicksman, M., Arkin, M., Napper, A. and Inglese, J., eds), pp. 5–7, Eli Lilly & Company and the National Center for Advancing Translational Sciences, Bethesda, MD
39 Patton, C., Thompson, S. and Epel, D. (2004) Some precautions in using chelators to buffer metals in biological solutions. Cell Calcium **35**, 427–431
40 Zhang, H., Thompson, J. and Prestwich, G. D. (2009) A scalable synthesis of the IP7 isomer, 5-PP-Ins(1,2,3,4,6)P5. Org. Lett. **11**, 1551–1554
41 Lin, H., Fridy, P. C., Ribeiro, A. A., Choi, J. H., Barma, D. K., Vogel, G., Falck, J. R., Shears, S. B., York, J. D. and Mayr, G. W. (2009) Structural analysis and detection of biological inositol pyrophosphates reveal that the family of VIP/diphosphoinositol pentakisphosphate kinases are 1/3-kinases. J. Biol. Chem. **284**, 1863–1872
42 Albert, C., Safrany, S. T., Bembenek, M. E., Reddy, K. M., Reddy, K. K., Falck, J. R., Bröcker, M., Shears, S. B. and Mayr, G. W. (1997) Biological variability in the structures of diphosphoinositol polyphosphates in *Dictyostelium discoideum* and mammalian cells. Biochem. J. **327**, 553–560
43 Barker, C. J., Wright, J., Hughes, P. J., Kirk, C. J. and Michell, R. H. (2004) Complex changes in cellular inositol phosphate complement accompany transit through the cell cycle. Biochem. J. **380**, 465–473
44 Caffrey, J. J., Safrany, S. T., Yang, X. and Shears, S. B. (2000) Discovery of molecular and catalytic diversity among human diphosphoinositol-polyphosphate phosphohydrolases. An expanding Nudt family. J. Biol. Chem. **275**, 12730–12736
45 Safrany, S. T., Caffrey, J. J., Yang, X., Bembenek, M. E., Moyer, M. B., Burkhart, W. A. and Shears, S. B. (1998) A novel context for the 'MutT' module, a guardian of cell integrity, in a diphosphoinositol polyphosphate phosphohydrolase. EMBO J. **17**, 6599–6607
46 Soboll, S., Scholz, R. and Heldt, H. W. (1978) Subcellular metabolite concentrations. Dependence of mitochondrial and cytosolic ATP systems on the metabolic state of perfused rat liver. Eur. J. Biochem. **87**, 377–390
47 Chamberlain, P. P., Qian, X., Stiles, A. R., Cho, J., Jones, D. H., Lesley, S. A., Grabau, E. A., Shears, S. B. and Spraggon, G. (2007) Integration of inositol phosphate signaling pathways via human ITPK1. J. Biol. Chem. **282**, 28117–28125
48 Saiardi, A., Erdjument-Bromage, H., Snowman, A. M., Tempst, P. and Snyder, S. H. (1999) Synthesis of diphosphoinositol pentakisphosphate by a newly identified family of higher inositol polyphosphate kinases. Curr. Biol. **9**, 1323–1326
49 Zhao, S., Snow, R. J., Stathis, C. G., Febbraio, M. A. and Carey, M. F. (2000) Muscle adenine nucleotide metabolism during and in recovery from maximal exercise in humans. J. Appl. Physiol. **88**, 1513–1519
50 Daniel, J. L., Robkin, L., Molish, I. R. and Holmsen, H. (1979) Determination of the ADP concentration available to participate in energy metabolism in an actin-rich cell, the platelet. J. Biol. Chem. **254**, 7870–7873
51 Fawaz, M. V., Topper, M. E. and Firestine, S. M. (2011) The ATP-grasp enzymes. Bioorg. Chem. **39**, 185–191
52 Saiardi, A., Nagata, E., Luo, H. R., Snowman, A. M. and Snyder, S. H. (2001) Identification and characterization of a novel inositol hexakisphosphate kinase. J. Biol. Chem. **276**, 39179–39185
53 Draškovič, P., Saiardi, A., Bhandari, R., Burton, A., Ilc, G., Kovačevič, M., Snyder, S. H. and Podobnik, M. (2008) Inositol hexakisphosphate kinase products contain diphosphate and triphosphate groups. Chem. Biol. **15**, 274–286
54 Schneider, C. A., Rasband, W. S. and Eliceiri, K. W. (2012) NIH Image to ImageJ: 25 years of image analysis. Nat. Meth. **9**, 671–675
55 Van Veldhoven, P. P. and Mannaerts, G. P. (1987) Inorganic and organic phosphate measurements in the nanomolar range. Anal. Biochem. **161**, 45–48

**Received 12 November 2012/7 December 2012; accepted 14 December 2012**

**Published as Immediate Publication 14 December 2012, doi 10.1042/BSR20120115**

Biosci. Rep. (2013) / **33** / art:e00022 / doi 10.1042/BSR20120115

OPEN ACCESS

Original Paper

## SUPPLEMENTARY DATA

# The kinetic properties of a human PPIP5K reveal that its kinase activities are protected against the consequences of a deteriorating cellular bioenergetic environment

Jeremy D. WEAVER, Huanchen WANG and Stephen B. SHEARS[1]

Inositol Signaling Group, Laboratory of Signal Transduction, National Institute of Environmental Health Sciences, NIH, DHHS, Research Triangle Park, P.O. Box 12233, NC 27709, U.S.A.

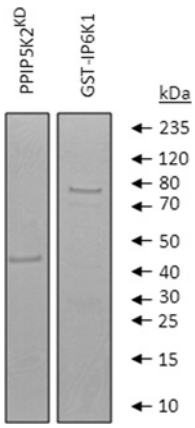


**Figure S1 Purity of recombinant enzymes**
SDS/PAGE of purified PPIP5K2$^{KD}$ and GST–IP6K1 (0.5 $\mu$g of protein/lane) stained with SimplyBlue SafeStain (Invitrogen). The maltose-binding protein and hexahistidine tags were cleaved by TEV (tobacco etch virus) protease from PPIP5K2$^{KD}$ during the purification procedure [1].

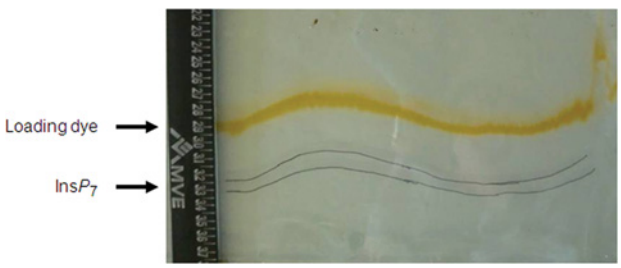


**Figure S2 Dye-front guided excision of *PP*-Ins*P***
Minor variations in the PAGE gel thickness cause uneven migration of the Orange G dye and *PP*-Ins*P*. A 1 cm-wide gel slice running the length of the gel was first stained with Toluidine Blue ([2]; results not shown) to reveal the location of the *PP*-Ins*P* relative to the dye front. The dye front was traced onto the glass, which was then used as a guide for excision of the *PP*-Ins*P* product after aligning the trace to the location of the *PP*-Ins*P* as revealed in the stained gel slice.

## REFERENCES

1 Wang, H., Falck, J. R., Hall, T. M. T. and Shears, S. B. (2012) Structural basis for an inositol pyrophosphate kinase surmounting phosphate crowding. Nat. Chem. Biol. **8**, 111–116
2 Loss, O., Azevedo, C., Szijgyarto, Z., Bosch, D. and Saiardi, A. (2011) Preparation of quality inositol pyrophosphates. J. Vis. Exp. e3027

**Received 12 November 2012/7 December 2012; accepted 14 December 2012**

**Published as Immediate Publication 14 December 2012, doi 10.1042/BSR20120115**

[1] To whom correspondence should be addressed (email Shears@niehs.nih.gov).